ACS Macro Letters

pubs.acs.org/macroletters

Viewpoint

Computational Phase Discovery in Block Polymers

Kevin D. Dorfman*

Cite This: ACS Macro Lett. 2024, 13, 1612−1619

Read Online

ACCESS | Metrics & More | Article Recommendations

ABSTRACT: Self-consistent field theory (SCFT), the mean-field theory of polymer thermodynamics, is a powerful tool for understanding ordered state selection in block copolymer melts and blends. However, the nonlinear governing equations pose a significant challenge when SCFT is used for phase discovery because converging an SCFT solution typically requires an initial guess close to the self-consistent solution. This Viewpoint provides a concise overview of recent efforts where machine learning methods (particle swarm optimization, Bayesian optimization, and generative adversarial networks) have been used to make the first strides toward converting SCFT from a primarily explanatory tool into one that can be readily deployed for phase discovery.

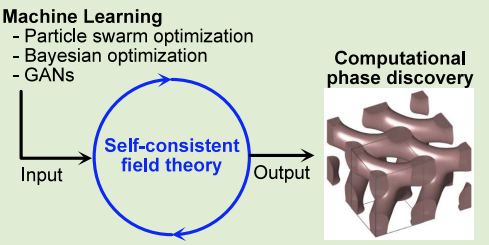

The long-standing scientific interest in block polymers arises, in part, from their ability to self-assemble into a vast number of ordered states from very simple building blocks. In contrast to self-assembly in other forms of soft matter, such as concentrated lipid solutions[1] or ligand-grafted nanoparticles,[2] the thermodynamics governing block copolymer self-assembly are a relatively simple combination of Gaussian chain statistics and Flory−Huggins interactions[3] applied to a single-component system. In light of this simplicity, the number of crystalline states that have been uncovered in block copolymers is remarkable. Consider the simplest case of a neat AB diblock copolymer melt. At equilibrium, depending on the A-block volume fraction, the ratio of the statistical segment lengths of the A and B blocks (the conformational asymmetry), and the segregation strength, an AB diblock copolymer can be in one of four particle-forming states (body-centered cubic (bcc),[4,5] close packed,[6] A15,[7] or σ[8]), two network phases (double gyroid[9] or the *Fddd* network[10] known as O^{70}), hexagonally close-packed cylinders, or lamellae.[11] Understanding the fundamental mechanisms giving rise to this phase behavior, let alone the massive number of phases that emerge in multiblock polymer melts[12,13] and various metastable states accessible by processing,[14−16] has been a decades-long effort in block polymer research.

Self-consistent field theory (SCFT) is the primary tool for computing the free energy of block polymer melts and thus interrogating their phase behavior. Readers interested in a pedagogical introduction to SCFT are referred to a recent primer[17] that provides an entry point to the more rigorous explanations in the literature.[3,18,19] Strictly speaking, SCFT is valid in the limit of an infinite invariant degree of polymerization $\bar{N}$, where $\bar{N}^{1/2}$ is the ratio of the pervaded volume of the chain to its self-volume.[20,21] In the mean-field limit $\bar{N} \to \infty$, the partition function is dominated by a single configuration of the fields, and SCFT refers to the computation of the resulting morphology and free energy. Like all field theories, SCFT becomes increasingly efficient with increasing density because (i) the many-bodied interactions are decoupled through the particle-to-field tranformation and (ii) the dynamics of the physical system are no longer important, so the calculations are much faster than, say, molecular dynamics simulations of a coarse-grained polymer model.[18] As a mean-field theory, SCFT cannot accurately predict the order−disorder transition (ODT);[22] the mean-field disordered state is homogeneous, but there exists structure in the disordered state proximate to the ODT[23−26] that can only be captured in theory through a fluctuating field model.[27,28] However, a comparison of calibrated particle-based simulation models to SCFT have revealed that the ordered-state free energies predicted by SCFT are remarkably close to those produced by simulations, even if the simulations are at values of $\bar{N}$ far from the mean-field limit.[29,30] Thus, provided that $\bar{N} \gtrsim 10^3$ and we are examining phase behavior above the ODT for that value of $\bar{N}$, the mean-field approximation embedded in SCFT is not a severe limitation for predicting the free energy.[29]

SCFT has played a key explanatory role in block polymer phase behavior. For example, SCFT calculations were essential to establishing the stability of double gyroid relative to double diamond and perforated lamellae,[31] as well as demonstrating that conformational asymmetry stabilizes the Frank−Kasper σ-phase.[32] While SCFT has been a crucial counterpart to experiments in explaining the origins of different ordered phases, the theory has played a much smaller role in the discovery of new phases. There are two notable exceptions: the

Received: September 30, 2024
Revised: November 4, 2024
Accepted: November 5, 2024
Published: November 12, 2024

predictions of a Frank−Kasper phase[33] and the O^{70} phase in diblock copolymers,[34] each of which were later realized experimentally.[7,8,10] While these two papers[33,34] shine as examples of phase discovery via SCFT, a theory-driven approach to block polymer phase discovery, akin to what has happened (either by design or serendipity) in experiments, remains an elusive goal.

Why is the computational phase discovery by SCFT so challenging? The answer lies in the SCFT workflow depicted in Figure 1. Initializing an SCFT calculation requires first

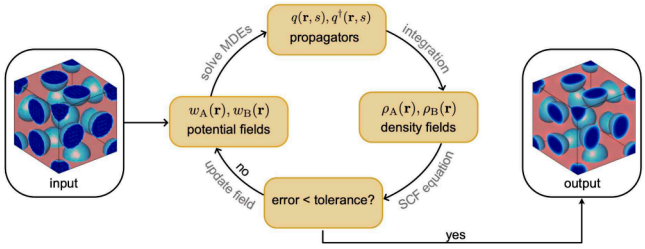

Figure 1. Illustration of the workflow for an SCFT calculation. In this example, the form-factor method was used to generate the initial guess (input) on the left. The converged solution with an optimal unit cell (output) is provided in the right-hand image. Reproduced with permission from ref 17. Copyright 2024 American Chemical Society.

generating an initial guess for the chemical potential fields. There are methods for generating these guesses based on the morphology of a system. For example, particle-forming phases can be initialized using a form-factor method,[35,36] and network phases are readily generated using level sets.[36,37] The solution then proceeds in an iterative manner:[17,18] (i) the constrained partition functions (also called the propagators) for each species are computed from the solution of the modified diffusion equations (MDEs) using the chemical potential fields; (ii) those propagators are used to compute the density fields for each block; (iii) the density fields are used to check the self-consistent field (SCF) equations; and (iv) if the chemical potential fields from step (iii) do not agree with the fields used for step (i), the chemical potential fields are updated for the next iteration. Depending on the quality of the initial guess, tens to hundreds of iterations are typically required and there is no guarantee of convergence. Therein lies the challenge when using SCFT for phase discovery: how can you find anything new if you have to have a good estimate of the answer to start the calculation?

A natural starting point for addressing this challenge is to start from many random initial guesses for the fields and attempt to converge them in parallel. This combinatorial approach, proposed by Drolet and Fredrickson in 1999,[38] was partially successful. They identified all of the equilibrium phases known at that time for diblock copolymers (bcc spheres, hexagonally packed cylinders, double gyroid, and lamellae) along with many defective, metastable solutions. The Drolet−Fredrickson approach used a simple mixing ("Picard-type algorithm") to evolve the chemical potential fields.[38] The advantage of this iterative algorithm is that it is tolerant to the quality of the initial guess, but the convergence rate is very slow[39,40] compared to more sophisticated methods such as Anderson mixing.[41] In the context of phase discovery, which is our focus here, it is notable that these calculations[38] produced neither the O^{70} network phase, an equilibrium state predicted by SCFT six years later,[34] nor the Frank−Kasper phases that have dominated the study of diblock copolymer phase behavior in recent years.[42] However, it is worth noting that both O^{70} and the Frank−Kasper phases have large unit cells that typically require many basis functions to resolve; it is unlikely that random initial guesses on a relatively coarse grid would produce, for example, the 30 particles in the Frank−Kasper σ-phase.[42] It is also possible that the absence of these phases in prior work[38] is simply the result of a limited number of calculations. Given sufficient computational resources and sufficiently large unit cells, it is reasonable to posit that random initialization would eventually produce SCFT calculations that converged to an O^{70} phase and various Frank−Kasper phases, as well as other novel phases.

If the convergence rate of a tolerant SCFT solver is the problem, then a potential solution is to abandon SCFT in favor of an approximate Hamiltonian while retaining the idea of random initialization. This approach, pursued by Bohovot-Raviv and Wang[43] shortly after the pioneering work of Drolet and Fredrickson,[38] appears to be robust at identifying interesting morphologies, at least for the ABC terpolymers in two dimensions studied in that paper.[43] Bohovot-Raviv and Wang further suggested that their approximate approach could be used to generate initial guesses for SCFT, a tantalizing idea that has not been pursued.

In the intervening 25 years, two major advances have revived recent interest in (and increased the feasibility of) using SCFT for computational phase discovery in block polymers beyond these two early examples.[38,43] The first advance is improvements in the numerical methods, including efficient algorithms for solving the modified diffusion equations for the propagators;[44] better algorithms for updating the chemical potential fields, most notably Anderson mixing[39,41] and semi-implicit methods;[18,45] and a method for computing the unit cell stress,[46] which can be incorporated with the self-consistent field update to accelerate the overall calculation.[47] Many of these methodological advances are available in the open-source Polymer Self-Consistent Field (PSCF) package from Morse and collaborators,[47,48] including a GPU implementation[49] that can be useful for large unit cell calculations such as Frank−Kasper phases.[50]

The second important advance has been the massive interest in machine learning (ML) and the applications of these methods to polymer science. Figure 2 outlines the different approaches that have been developed in the context of the phase behavior. The ideal situation (Figure 2a) is to go directly from the polymer formulation to the prediction of the phase. Given sufficient data, some (or all) of which could come from SCFT, this is a reasonable proposal but one that has been only partially realized to date,[52−58] in part because the amount of available data is much smaller than, for example, scraping the internet for image data to train ML to generate new images. A second approach (Figure 2b) is to use ML to accelerate the SCFT calculations by removing the main bottleneck, namely, solving the modified diffusion equations for the propagators. This is an active area of investigation[59−63] and likely to prove fruitful in the coming years. For the purposes of phase discovery, however, the most useful immediate application of ML for SCFT is the generation of nonobvious initial guesses (Figure 2c) that will converge to previously unanticipated phases. The advantage of ML here is that the demands placed on the guess generator are modest because the converged SCFT solution ensures that the result is physically relevant; the generator simply needs to provide initial conditions in different basins of attraction that will converge to different SCFT fixed points.[51] While we have posed the methods in Figure 2 as distinct approaches, in the long run, they should all

https://doi.org/10.1021/acsmacrolett.4c00661
ACS Macro Lett. 2024, 13, 1612−1619

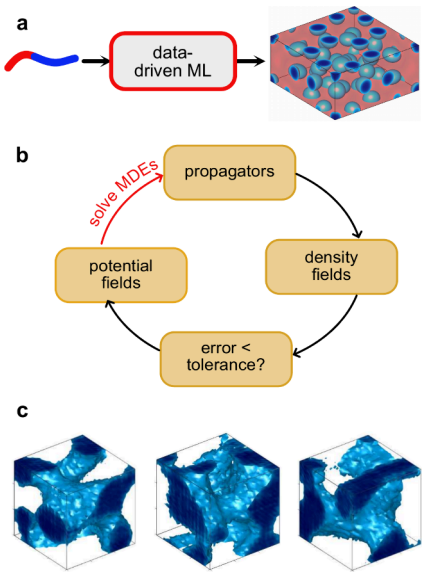

Figure 2. Approaches to using machine learning to enable block polymer phase discovery. (a) Data-driven methods that go directly from the polymer formulation and the temperature to the predicted phase. (b) Use of machine learning methods, such as neural networks, for solving the modified diffusion equations (MDEs), which are the bottleneck in the SCFT calculation. (c) Use of machine learning methods to generate initial guesses that will converge to different solutions. The structures in this panel converged to O[52], O[70], and hexagonally perforated lamellae. The structure in panel (a) and the algorithm in panel (b) were adapted from ref 17. Copyright 2024 American Chemical Society. Initial guesses in panel (c) were adapted from ref 51. Copyright 2023 the authors.

be synergistic: fast ML methods to solve the SCFT equations (Figure 2b) can be used to converge novel initial guesses (Figure 2c) with high throughput, thereby generating sufficient data to ultimately produce a data-driven approach to directly predicting phase behavior from the polymer properties without the intermediate step of computing free energies (Figure 2a). Alternatively, the novel initial guesses can be used as candidate phases in an inverse design approach to determine polymer formulations that can stabilize a new morphology.

To date there have been three approaches to using ML to generate fruitful initial guesses for SCFT. The first two use different stochastic optimization approaches, either particle swarm optimization (PSO)[64] or Bayesian optimization.[65] The third is a different direction using generative adversarial networks (GANs)[51] that learn from SCFT trajectories.

In PSO, a set of agents move in a convective-diffusive manner, where the convective term is based on information received from other agents to drive them toward a more promising region of the space, the swarming, while the random (diffusive) part enables escape from local minima.[66] The overall dynamics are intended to mimic, for example, the way insects search for food. Early applications of PSO to block polymer phase behavior focused on the inverse design problem, where the agents move in the state space (e.g., block volume fraction and segregation strength) in response to comparisons of the free energy of a target phase relative to other possible phases.[67−69] These early works cannot be considered phase discovery, however, since all of the possible phases need to be itemized *a priori* to compute the fitness.

The first example of using PSO for phase discovery is the work by Tsai and Fredrickson.[64] As illustrated in the example of Figure 3, the agents are randomly initialized as pairs of peaks in a thin shell of radius q^* in reciprocal space, where q^* is the primary peak in the structure factor. This approach thus shares a methodological lineage with the pioneering study by Drolet and Fredrickson[38] because the initialization method is random, but now with a sparser set of information (pairs of peaks) and a switch from real space to reciprocal space. The SCFT calculation is then initialized with chemical potential fields that correspond to the structure factor produced by those peaks. The fitness used for PSO is the free energy produced by the converged SCFT solution, and the agents are evolved via PSO to new values of the peak positions, peak amplitudes, and value of q^*. The PSO trajectory in Figure 3 is a clear example of phase discovery, as the

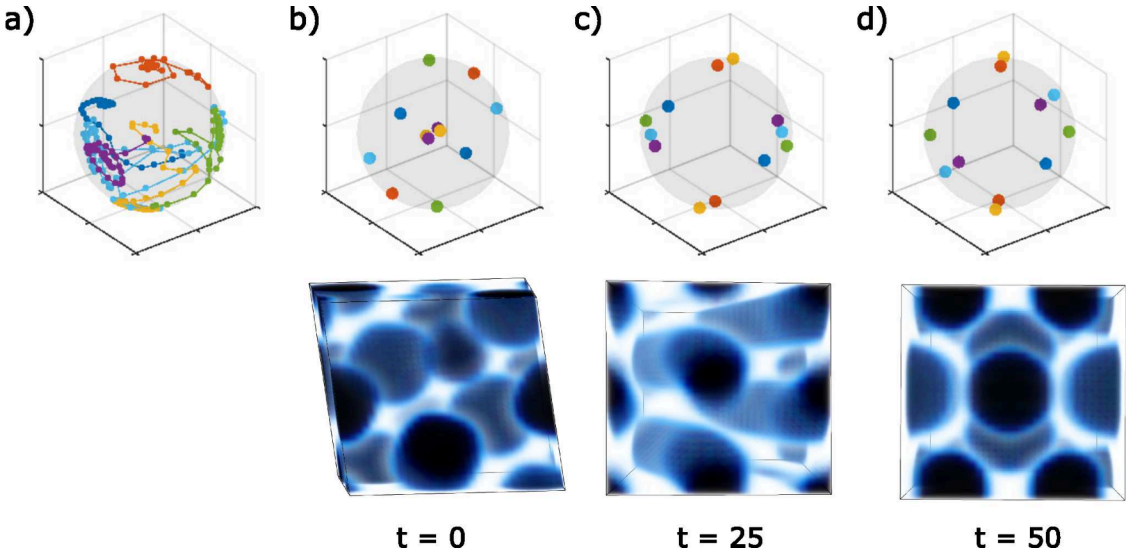

Figure 3. Example of using particle swarm optimization (PSO) for phase discovery, where the agents are pairs of peaks on a thin shell in reciprocal space around the primary peak q^*. (a) Trajectory of the agents during the PSO. Only one of each pair of peaks is illustrated. (b−d) Location of the agents in reciprocal space and the SCFT morphology from the converged solution for iterations 0, 25, and 50. Reproduced with permission from ref 64. Copyright 2022 American Chemical Society.

https://doi.org/10.1021/acsmacrolett.4c00661
ACS Macro Lett. 2024, 13, 1612−1619

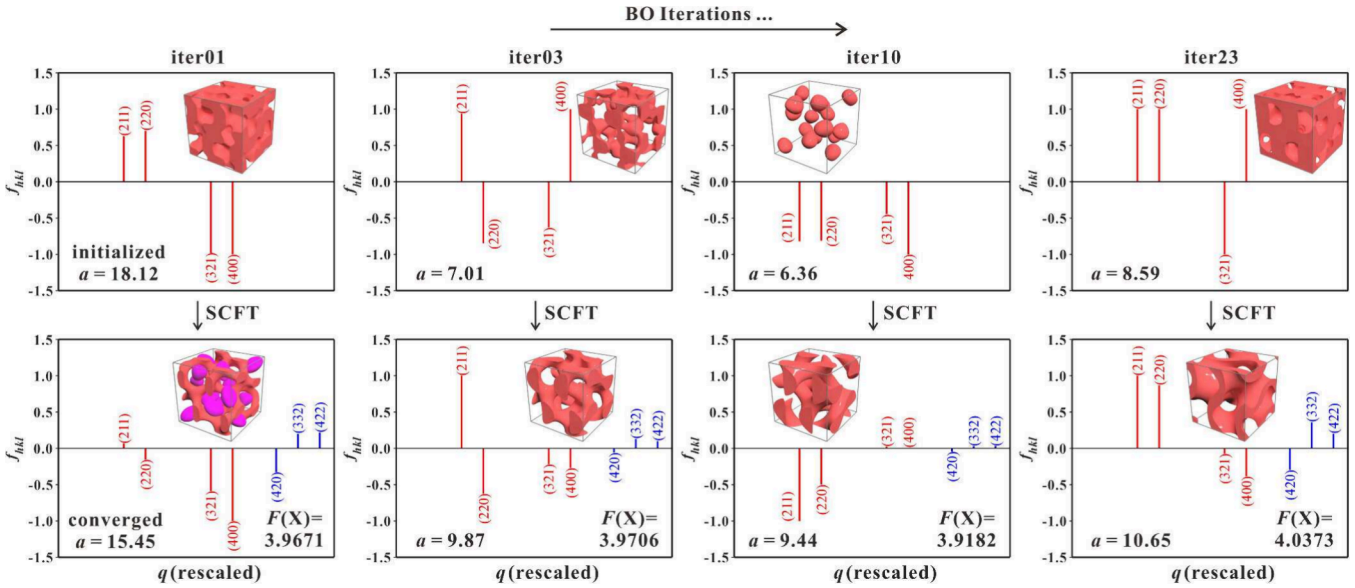

Figure 4. Example of Bayesian optimization applied to a surrogate model for the first four basis functions in a symmetry-constrained basis set for space group $Im\bar{3}d$ (red). At each iteration, an SCFT calculation produces a value of the free energy $F(X)$ and optimized cubic unit cell parameter a that is used to update the surrogate model. The blue peaks in the SCFT calculation correspond to the weights of the next few symmetry-constrained basis functions, and the changes in the intensity of the red peaks are the adjustments in the low q wavevectors during the SCFT calculation. Reproduced with permission from ref 65. Copyright 2024 American Chemical Society.

structure after 50 iterations of PSO was deemed a "mystery" phase by the authors and thus not anticipated.[64] Remarkably, this structure is the Frank−Kasper Z-phase, which was considered as a possible candidate phase in previous work on Laves phases in diblock copolymer melts[15] and has been produced in giant shape amphiphiles.[70]

The other optimization approach used for phase discovery is Bayesian optimization.[71] Bayesian optimization requires two inputs: (i) a probabilistic surrogate model that describes the current belief in the value of the objective function for a given set of inputs and (ii) an acquisition function that quantifies the optimality of a sequence of queries. In each iteration of Bayesian optimization, the next evaluation of the objective function (the query) is based on the acquisition function, and the query is selected to maximize the amount of information that is learned about the objective function. The output of that query is then used to update the surrogate model with new information. Each iteration thus decreases the uncertainty in the surrogate model.

Dong et al.[65] merged Bayesian optimization with SCFT by using a small set of symmetry-constrained basis functions for the SCFT initialization step, where the Bayesian optimization parameters are the weights for each basis function and the cubic unit cell parameter. The surrogate model is a Gaussian process model for the lower bound confidence of the free energy, whereupon the Bayesian optimization selects queries (values of the basis function weights and the unit cell parameter) that reduce the uncertainty in the dependence of the free energy on those parameters. Importantly, for a pseudospectral SCFT calculation, the number of basis functions is equal to the number of grid points. As a result, the SCFT calculation has more information than the surrogate model; including all of that information in the surrogate model would be prohibitively expensive, because it would create a search in a much higher dimensional space.

As we can see in the example in Figure 4, the weights for the basis functions in the surrogate model are adjusted by the Bayesian optimization model during each iteration. Since each Bayesian optimization step produces a new converged SCFT solution, each iteration corresponds to a possible candidate phase in that space group. While the equilibrium phase is the one with the lowest free energy, the goal here is phase exploration. In this sense, the advantage of Bayesian optimization is that the acquisition function continuously suggests a new point in the basis function space for computation that will reduce the uncertainty in the free energy model and that reduction is likely to be a place where there is a novel phase (because the free energy of that region of the space is very uncertain *a priori*). As such, the generation of candidate phases is somewhat decoupled from the free energy optimization in the sense that subsequent queries do not necessarily need to be lower free energy states.

In both the Bayesian optimization[65] and the PSO[64] approaches, the search space is reduced by either restricting the initialization to be symmetry-constrained basis vectors[65] or wave vectors of approximate magnitude q^*.[64] Both approaches reduce the dimensionality of the search space compared to the full basis set used for the SCFT calculation, and they have a further benefit of removing local free energy minima that emerge from the roughness of the free energy when all basis functions are included.[65] However, each approach has its drawbacks. When restricting the basis functions to a shell at q^*, there is no way for the system to converge on a solution that has strong peaks in the structure function with very different values of q, such as the σ phase.[65] This limitation is removed by using symmetry-constrained basis functions. However, if one only uses symmetry-constrained basis functions, then the structures that emerge from the calculation all have the same symmetry; therefore, the Bayesian optimization-SCFT calculation needs to be repeated for every space group. Moreover, for low symmetry space groups, many basis functions are required, and the advantage of using symmetry-constrained basis functions is reduced.

The third approach, which uses generative adversarial networks (GANs) to generate the initial guesses, is quite different from the preceding optimization-based methods. A

https://doi.org/10.1021/acsmacrolett.4c00661
ACS Macro Lett. 2024, 13, 1612−1619

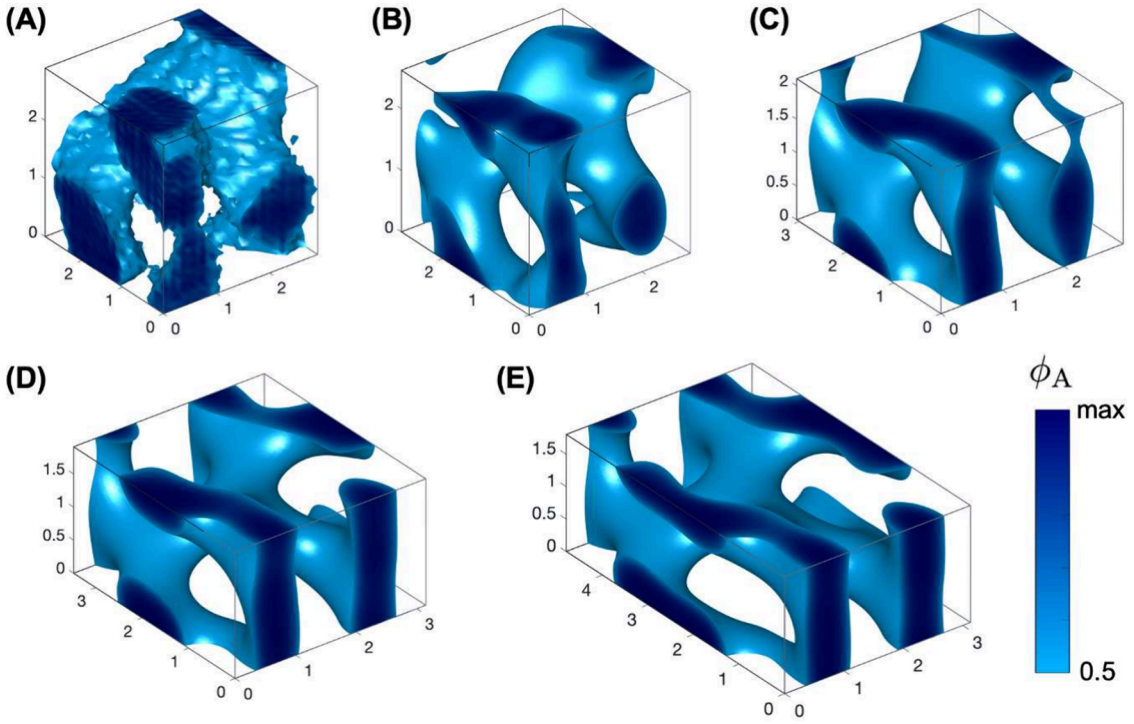

Figure 5. Discovery of the H[181] network phase using a generative adversarial network (GAN) for initial guess generation. The different panels show the trajectory of the SCFT solution from (a) the initial guess to (b) 11, (c) 33, (d) 65, and (e) 266 iterations. The axis tick marks correspond to the unit cell size in units of the diblock polymer's end-to-end distance. The maximum value of the color bar differs for each panel and they are available in ref 51. Reproduced from ref 51. Copyright 2023 the authors.

GAN[72,73] uses two neural networks, a generator and a discriminator. The generator takes as input random noise and returns examples. The discriminator compares those examples to a set of true data and assesses whether the output of the discriminator is real or fake. Both networks are trained in tandem to improve their performance. In a converged GAN, the discriminator cannot tell the difference between the fake data and real data. GANs have been used, most famously, for generating fake pictures from a set of real images. Such applications put a high demand on the GAN because the output of the generator, in the end, must fool a human discriminator.

In the context of SCFT, the demands on the generator are much lower because the initial guesses simply need to be "good enough" for SCFT to converge them to a physically relevant solution. The key is to have sufficient diversity in the initial guesses produced by the GAN so that new phases emerge. In our work,[51] we trained the GAN with SCFT trajectory data from five network phases (single gyroid, double gyroid, single diamond, single primitive and double primitive) at a state point where a diblock copolymer melt produces double gyroid as the stable state.[31] The approach not only uncovered every known network phase in block polymers,[10,74−76] but ended up producing a total of 349 candidate phases with competitive free energies.

Figure 5 shows the SCFT trajectory that produced the most intriguing of those candidate phases, H[181]. The free energy of H[181] lies slightly below hexagonally perforated lamellae, which has been produced in diblock polymers via processing.[74,75] From a materials science standpoint, H[181] is notable for its chiral network,[51,77] which could endow it with useful optical properties. From a methodological standpoint, Figure 5 demonstrates the remarkable ability of SCFT to modulate the structure during the calculation, including large changes in the unit cell dimensions due to stress relaxation, which reinforces the claim that the demands placed on the generator are modest. Importantly, H[181] has not been observed or considered previously in soft matter, demonstrating the power of a GAN to generate novel results.

The approach we pursued[51] simply represents the first step toward the use of GANs for block polymer phase discovery, and there are numerous avenues for improvement.[78] Indeed, the precise reason for the success of the GAN approach in our study[51] is unclear; as is the case with many machine-learning methods, interpretability is not simple. However, we suspect that two key factors play a role. First, the training data provides the GAN with information about both cocontinuous phases and known network topologies, which should allow it to infer similar structures as initial guesses. Second, the dynamics of an SCFT trajectory using Anderson mixing to simultaneously relax the unit cell stress and solve for the saddle point of the fields[47] is disconnected from any physical relaxation mechanism such as Rouse diffusion. As a result, even when starting from initial guesses that are reasonably far from the fixed point, as is the case in Figure 5, the SCFT iterator can impose large-scale changes to the structure that can ultimately converge to a crystal structure that may have only minimal similarity to the initial condition.

The adoption of machine-learning methods to improve phase discovery in block copolymers is clearly in its infancy, but the results so far are promising.[51,64,65] Understandably, most of the focus to date has been on systems where the phase behavior is already well understood, in particular, for AB diblock copolymers, demonstrating that all of the known phases can be generated and that previously unanticipated solutions to the SCFT equations emerge. Since these are well studied polymer systems, it is unsurprising (but also unfortunate) that no new stable states have been discovered akin to what was done in predicting the existence of a Frank−Kasper phase in branched

https://doi.org/10.1021/acsmacrolett.4c00661
ACS Macro Lett. 2024, 13, 1612−1619

diblocks[33] or the prediction of the O^{70} phase in linear diblock copolymers near the ODT.[34] Finding new stable morphologies will require extending these methods to more complicated architectures or to block polymer blends (or both), which may prove nontrivial from a methodological standpoint. Moreover, increasing the state space (block volume fractions, segregation strengths, and blend composition) will likely require that inverse design tools, such as PSO[67−69] or Bayesian optimization,[79] be deployed in conjunction with initial guess generators to efficiently search through the state space for novel, stable solutions. These searches will require (at least) tens to hundreds of thousands of SCFT calculations, which will place computational demands that have been met in part through GPU acceleration[49,50] and could be further improved, at least in principle, through machine learning advances for solving the modified diffusion equations.[59−63] While there is work to be done, there is now a clear path forward for converting SCFT from a primarily explanatory tool into a truly predictive tool.

AUTHOR INFORMATION

Corresponding Author

Kevin D. Dorfman − *Department of Chemical Engineering and Materials Science, University of Minnesota−Twin Cities, Minneapolis, Minnesota 55455, United States;* orcid.org/0000-0003-0065-5157; Email: dorfman@umn.edu

Complete contact information is available at: https://pubs.acs.org/10.1021/acsmacrolett.4c00661

Notes

The author declares no competing financial interest.

ACKNOWLEDGMENTS

This work was supported primarily by the National Science Foundation through the University of Minnesota MRSEC under Award Number DMR-2011401. I thank Guo-Kang Cheong and Pengyu Chen for discussions related to these topics.

REFERENCES

(1) Mezzenga, R.; Seddon, J. M.; Drummond, C. J.; Boyd, B. J.; Schröder-Turk, G. E.; Sagalowicz, L. Nature-Inspired Design and Application of Lipidic Lyotropic Liquid Crystals. *Adv. Mater.* **2019**, *31*, 1900818.

(2) Boles, M. A.; Engel, M.; Talapin, D. V. Self-Assembly of Colloidal Nanocrystals: From Intricate Structures to Functional Materials. *Chem. Rev.* **2016**, *116*, 11220−11289.

(3) Matsen, M. W. The Standard Gaussian Model for Block Copolymer Melts. *J. Phys.: Condens. MatterJ. Phys.: Condens. Matter* **2002**, *14*, R21−R47.

(4) Bates, F. S.; Cohen, R. E.; Berney, C. V. Small-Angle Neutron Scattering Determination of Macrolattice Structure in a Polystyrene-Polybutadiene Diblock Copolymer. *Macromolecules* **1982**, *15*, 589−592.

(5) Thomas, E. L.; Kinning, D. J.; Alward, D. B.; Henkee, C. S. Ordered Packing Arrangements of Spherical Micelles of Diblock Copolymers in Two and Three Dimensions. *Macromolecules* **1987**, *20*, 2934−2939.

(6) Huang, Y. Y.; Hsu, J. Y.; Chen, H. L.; Hashimoto, T. Existence of Fcc-Packed Spherical Micelles in Diblock Copolymer Melt. *Macromolecules* **2007**, *40*, 406−409.

(7) Bates, M. W.; Lequieu, J.; Barbon, S. M.; Lewis, R. M., III; Delaney, K. T.; Anastasaki, A.; Hawker, C. J.; Fredrickson, G. H.; Bates, C. M. Stability of the A15 Phase in Diblock Copolymer Melts. *Proc. Natl. Acad. Sci. U.S.A.* **2019**, *116*, 13194−13199.

(8) Lee, S.; Bluemle, M. J.; Bates, F. S. Discovery of a Frank-Kasper σ Phase in Sphere-Forming Block Copolymer Melts. *Science* **2010**, *330*, 349−353.

(9) Hajduk, D. A.; Harper, P. E.; Gruner, S. M.; Honeker, C. C.; Kim, G.; Thomas, E. L.; Fetters, L. J. The Gyroid: A New Equilibrium Morphology in Weakly Segregated Diblock Copolymers. *Macromolecules* **1994**, *27*, 4063−4075.

(10) Takenaka, M.; Wakada, T.; Akasaka, S.; Nishitsuji, S.; Saijo, K.; Shimizu, H.; Kim, M. I.; Hasegawa, H. Orthorhombic Fddd Network in Diblock Copolymer Melts. *Macromolecules* **2007**, *40*, 4399−4402.

(11) Kämpf, G.; Hoffmann, M.; Krömer, H. Conformation, supermolecular structure and long-range ordering in noncrystalline and nonstereospecific polymers Part I. Visible supermolecular structures and long-range ordering in noncrystalline block copolymers. *Ber. Bunsenges. Phys. Chem.* **1970**, *74*, 851−859.

(12) Meuler, A. J.; Hillmyer, M. A.; Bates, F. S. Ordered Network Mesostructures in Block Polymer Materials. *Macromolecules* **2009**, *42*, 7221−7250.

(13) Bates, C. M.; Bates, F. S. 50th Anniversary Perspective: Block Polymers−Pure Potential. *Macromolecules* **2017**, *50*, 3−22.

(14) Cochran, E. W.; Bates, F. S. Shear-Induced Network-to-Network Transition in a Block Copolymer Melt. *Phys. Rev. Lett.* **2004**, *93*, 087802.

(15) Kim, K.; Schulze, M. W.; Arora, A.; Lewis, R. M., III; Hillmyer, M. A.; Dorfman, K. D.; Bates, F. S. Thermal Processing of Diblock Copolymer Melts Mimics Metallurgy. *Science* **2017**, *356*, 520−523.

(16) Kim, K.; Arora, A.; Lewis, R. M., III; Liu, M.; Li, W.; Shi, A.-C.; Dorfman, K. D.; Bates, F. S. Origins of Low-Symmetry Phases in Asymmetric Diblock Copolymer Melts. *Proc. Natl. Acad. Sci. U.S.A.* **2018**, *115*, 847−854.

(17) Magruder, B. R.; Dorfman, K. D. *Theory of Block Polymer Self-Assembly*; American Chemical Society, 2024, .

(18) Fredrickson, G. H. *The Equilibrium Theory of Inhomogeneous Polymers*; Clarendon Press: Oxford, 2006.

(19) Shi, A.-C. Self-Consistent Field Theory of Inhomogeneous Polymeric Systems: A Variational Derivation. *Adv. Theory Simul.* **2019**, *2*, 1800188.

(20) Fredrickson, G. H.; Helfand, E. Fluctuation Effects in the Theory of Microphase Separation in Block Copolymers. *J. Chem. Phys.* **1987**, *87*, 697−705.

(21) Glaser, J.; Medapuram, P.; Beardsley, T. M.; Matsen, M. W.; Morse, D. C. Universality of Block Copolymer Melts. *Phys. Rev. Lett.* **2014**, *113*, 068302.

(22) Khandpur, A. K.; Förster, S.; Bates, F. S.; Hamley, I. W.; Ryan, A. J.; Bras, W.; Almdal, K.; Mortensen, K. Polyisoprene-Polystyrene Diblock Copolymer Phase Diagram near the Order-Disorder Transition. *Macromolecules* **1995**, *28*, 8796−8806.

(23) Bates, F. S.; Rosedale, J. H.; Fredrickson, G. H. Fluctuation Effects in a Symmetric Diblock Copolymer near the Order-Disorder Transition. *J. Chem. Phys.* **1990**, *92*, 6255−6270.

(24) Kim, J. K.; Lee, H. H.; Sakurai, S.; Aida, S.; Masamoto, J.; Nomura, S.; Kitagawa, Y.; Suda, Y. Lattice Disordering and Domain Dissolution Transitions in Polystyrene-Block-Poly(Ethylene-Co-but-1-Ene)-Block-Polystyrene Triblock Copolymer Having a Highly Asymmetric Composition. *Macromolecules* **1999**, *32*, 6707−6717.

(25) Han, C. D.; Vaidya, N. Y.; Kim, D.; Shin, G.; Yamaguchi, D.; Hashimoto, T. Lattice Disordering/Ordering and Demicellization/Micellization Transitions in Highly Asymmetric Polystyrene-Block-Polyisoprene Copolymers. *Macromolecules* **2000**, *33*, 3767−3780.

(26) Vidil, T.; Hampu, N.; Hillmyer, M. A. Nanoporous Thermosets with Percolating Pores from Block Polymers Chemically Fixed above the Order-Disorder Transition. *ACS Central Sci.* **2017**, *3*, 1114−1120.

(27) Delaney, K. T.; Fredrickson, G. H. Recent Developments in Fully Fluctuating Field-Theoretic Simulations of Polymer Melts and Solutions. *J. Phys. Chem. B* **2016**, *120*, 7615−7634.

(28) Matsen, M. W.; Beardsley, T. M.; Willis, J. D. Fluctuation-Corrected Phase Diagrams for Diblock Copolymer Melts. *Phys. Rev. Lett.* **2023**, *130*, 248101.

(29) Medapuram, P.; Glaser, J.; Morse, D. C. Universal Phenomenology of Symmetric Diblock Copolymers near the Order-Disorder Transition. *Macromolecules* **2015**, *48*, 819−839.
(30) Ghasimakbari, T.; Morse, D. C. Order-Disorder Transitions and Free Energies in Asymmetric Diblock Copolymers. *Macromolecules* **2020**, *53*, 7399−7409.
(31) Matsen, M. W.; Schick, M. Stable and Unstable Phases of a Diblock Copolymer Melt. *Phys. Rev. Lett.* **1994**, *72*, 2660−2663.
(32) Xie, N.; Li, W.; Qiu, F.; Shi, A.-C. σ Phase Formed in Conformationally Asymmetric AB-Type Block Copolymers. *ACS Macro Lett.* **2014**, *3*, 906−910.
(33) Grason, G. M.; DiDonna, B. A.; Kamien, R. D. Geometric Theory of Diblock Copolymer Phases. *Phys. Rev. Lett.* **2003**, *91*, 058304.
(34) Tyler, C. A.; Morse, D. C. Orthorhombic Fddd Network in Triblock and Diblock Copolymer Melts. *Phys. Rev. Lett.* **2005**, *94*, 208302.
(35) Xu, W.; Jiang, K.; Zhang, P.; Shi, A.-C. A Strategy to Explore Stable and Metastable Ordered Phases of Block Copolymers. *J. Phys. Chem. B* **2013**, *117*, 5296−5305.
(36) Arora, A.; Qin, J.; Morse, D. C.; Delaney, K. T.; Fredrickson, G. H.; Bates, F. S.; Dorfman, K. D. Broadly Accessible Self-Consistent Field Theory for Block Polymer Materials Discovery. *Macromolecules* **2016**, *49*, 4675−4690.
(37) Cochran, E. W. Thermodynamics Simulation, and Modeling of Ordered Linear ABC Triblock Copolymers *Ph.D. thesis*, University of Minnesota, Minneapolis, MN, 2004.
(38) Drolet, F.; Fredrickson, G. Combinatorial Screening of Complex Block Copolymer Assembly with Self-Consistent Field Theory. *Phys. Rev. Lett.* **1999**, *83*, 4317−4320.
(39) Thompson, R. B.; Rasmussen, K.; Lookman, T. Improved Convergence in Block Copolymer Self-Consistent Field Theory by Anderson Mixing. *J. Chem. Phys.* **2004**, *120*, 31−34.
(40) Stasiak, P.; Matsen, M. W. Efficiency of Pseudo-Spectral Algorithms with Anderson Mixing for the SCFT of Periodic Block-Copolymer Phases. *Eur. Phys. J. E* **2011**, *34*, 110.
(41) Matsen, M. W. Fast and Accurate SCFT Calculations for Periodic Block-Copolymer Morphologies Using the Spectral Method with Anderson Mixing. *Eur. Phys. J. E* **2009**, *30*, 361−369.
(42) Dorfman, K. D. Frank-Kasper Phases in Block Polymers. *Macromolecules* **2021**, *54*, 10251−10270.
(43) Bohbot-Raviv, Y.; Wang, Z.-G. Discovering New Ordered Phases of Block Copolymers. *Phys. Rev. Lett.* **2000**, *85*, 3428−3431.
(44) Ranjan, A.; Qin, J.; Morse, D. C. Linear Response and Stability of Ordered Phases of Block Copolymer Melts. *Macromolecules* **2008**, *41*, 942−954.
(45) Ceniceros, H. D.; Fredrickson, G. H. Numerical Solution of Polymer Self-Consistent Field Theory. *Multiscale Model Sim.* **2004**, *2*, 452−474.
(46) Tyler, C. A.; Morse, D. C. Stress in Self-Consistent-Field Theory. *Macromolecules* **2003**, *36*, 8184−8188.
(47) Arora, A.; Morse, D. C.; Bates, F. S.; Dorfman, K. D. Accelerating Self-Consistent Field Theory of Block Polymers in a Variable Unit Cell. *J. Chem. Phys.* **2017**, *146*, 244902.
(48) Morse, D. C., Collanton, R. P., Magruder, B. R., Chawla, A., Zheng, Y., Chen, K., Cheong, G.-K. Polymer Self-Consistent Field (PSCF). https://github.com/dmorse/pscfpp.
(49) Delaney, K. T.; Fredrickson, G. H. Polymer Field-Theory Simulations on Graphics Processing Units. *Comput. Phys. Commun.* **2013**, *184*, 2102−2110.
(50) Cheong, G. K.; Chawla, A.; Morse, D. C.; Dorfman, K. D. Open-Source Code for Self-Consistent Field Theory Calculations of Block Polymer Phase Behavior on Graphics Processing Units. *Eur. Phys. J. E* **2020**, *43*, 15.
(51) Chen, P.; Dorfman, K. D. Gaming Self-Consistent Field TheoryGenerative Block Polymer Phase Discovery. *Proc. Natl. Acad. Sci. U.S.A.* **2023**, *120*, e2308698120.
(52) Nakamura, I. Phase Diagrams of Polymer-Containing Liquid Mixtures with a Theory-Embedded Neural Network. *New J. Phys.* **2020**, *22*, 015001.
(53) Aoyagi, T. Deep Learning Model for Predicting Phase Diagrams of Block Copolymers. *Computer Mater. Sci.* **2021**, *188*, 110224.
(54) Zhao, S.; Cai, T.; Zhang, L.; Li, W.; Lin, J. Autonomous Construction of Phase Diagrams of Block Copolymers by Theory-Assisted Active. *ACS Macro Lett.* **2021**, *10*, 598−602.
(55) Arora, A.; Lin, T.-S.; Rebello, N. J.; Av-Ron, S. H. M.; Mochigase, H.; Olsen, B. D. Random Forest Predictor for Diblock Copolymer Phase Behavior. *ACS Macro Lett.* **2021**, *10*, 1339−1345.
(56) Wei, D.; Zhou, T.; Huang, Y.; Jiang, K. A Multi-Category Inverse Design Neural Network and Its Application to Diblock Copolymers. *Mathematics* **2022**, *10*, 4451.
(57) Rebello, N. J.; Arora, A.; Mochigase, H.; Lin, T.-S.; Shi, J.; Audus, D. J.; Muckley, E. S.; Osmani, A.; Olsen, B. D. The Block Copolymer Phase Behavior Database. *J. Chem. Inf. Model.* **2024**, *64*, 6464−6476.
(58) Hiraide, K.; Oya, Y.; Hirayama, K.; Endo, K.; Muramatsu, M. Development of a Deep-Learning Model for Phase-Separation Structure of Diblock Copolymer Based on Self-Consistent Field Analysis. *Adv. Compos. Mater.* **2024**, *33*, 1026.
(59) Wei, Q.; Jiang, Y.; Chen, J. Z. Y. Machine-Learning Solver for Modified Diffusion Equations. *Phys. Rev. E* **2018**, *98*, 053304.
(60) Xuan, Y.; Delaney, K. T.; Ceniceros, H. D.; Fredrickson, G. H. Deep Learning and Self-Consistent Field Theory: A Path towards Accelerating Polymer Phase Discovery. *J. Comput. Phys.* **2021**, *443*, 110519.
(61) Lin, D.; Yu, H.-Y. Deep Learning and Inverse Discovery of Polymer Self-Consistent Field Theory Inspired by Physics-Informed Neural Networks. *Phys. Rev. E* **2022**, *106*, 014503.
(62) Yong, D.; Kim, J. U. Accelerating Langevin Field-Theoretic Simulation of Polymers with Deep Learning. *Macromolecules* **2022**, *55*, 6505−6515.
(63) Xuan, Y.; Delaney, K. T.; Ceniceros, H. D.; Fredrickson, G. H. Machine Learning and Polymer Self-Consistent Field Theory in Two Spatial Dimensions. *J. Chem. Phys.* **2023**, *158*, 144103.
(64) Tsai, C. L.; Fredrickson, G. H. Using Particle Swarm Optimization and Self-Consistent Field Theory to Discover Globally Stable Morphologies of Block Copolymers. *Macromolecules* **2022**, *55*, 5249−5262.
(65) Dong, Q.; Xu, Z.; Song, Q.; Qiang, Y.; Cao, Y.; Li, W. Automated Search Strategy for Novel Ordered Structures of Block Copolymers. *ACS Macro Lett.* **2024**, *13*, 987−993.
(66) Kennedy, J., Eberhart, R. Particle Swarm Optimization. *Proceedings of ICNN'95 - International Conference on Neural Networks*, Perth, WA, Australia, Nov 27−Dec 1, 1995,IEEE, 1995, pp 1942−1948 DOI: 10.1109/ICNN.1995.488968.
(67) Paradiso, S. P.; Delaney, K. T.; Fredrickson, G. H. A Swarm Intelligence Platform for Multiblock Polymer Inverse Design. *ACS Macro Lett.* **2016**, *5*, 972−976.
(68) Khadilkar, M. R.; Paradiso, S.; Delaney, K. T.; Fredrickson, G. H. Inverse Design of Bulk Morphologies in Multiblock Polymers Using Particle Swarm Optimization. *Macromolecules* **2017**, *50*, 6702−6709.
(69) Case, L. J.; Delaney, K. T.; Fredrickson, G. H.; Bates, F. S.; Dorfman, K. D. Open-Source Platform for Block Polymer Formulation Design Using Particle Swarm Optimization. *Eur. Phys. J. E* **2021**, *44*, 115.
(70) Su, Z.; Hsu, C.-h.; Gong, Z.; Feng, X.; Huang, J.; Zhang, R.; Wang, Y.; Mao, J.; Wesdemiotis, C.; Li, T.; Seifert, S.; Zhang, W.; Aida, T.; Huang, M.; Cheng, S. Z. D. Identification of a Frank-Kasper Z Phase from Shape Amphiphile Self-Assembly. *Nat. Chem.* **2019**, *11*, 899−905.
(71) Shahriari, B.; Swersky, K.; Wang, Z.; Adams, R. P.; De Freitas, N. Taking the Human Out of the Loop: A Review of Bayesian Optimization. *Proc. IEEE* **2016**, *104*, 148−175.
(72) Goodfellow, I. J.; Pouget-Abadie, J.; Mirza, M.; Xu, B.; Warde-Farley, D.; Ozair, S.; courville, A.; Bengio, Y. Generative Adversarial Nets. *Advances in Neural Information Processing Systems* **2014**, *27*, 2672−2680.
(73) Radford, A.; Metz, L.; Chintala, S. Unsupervised Representation Learning with Deep Convolutional Generative Adversarial Networks. *4th International Conference on Learning Representations ICLR 2016 -*

Conference Track Proceedings, San Juan, Puerto Rico, May 2−4, 2016, DBLP, 2016, pp 1−16.
(74) Hamley, I. W.; Koppi, K. A.; Rosedale, J. H.; Bates, F. S.; Almdal, K.; Mortensen, K. Hexagonal Mesophases between Lamellae and Cylinders in a Diblock Copolymer Melt. *Macromolecules* **1993**, *26*, 5959−5970.
(75) Bates, F. S.; Schulz, M. F.; Khandpur, A. K.; Förster, S.; Rosedale, J. H.; Almdal, K.; Mortensen, K. Fluctuations, Conformational Asymmetry and Block Copolymer Phase Behaviour. *Faraday Disc.* **1994**, *98*, 7−18.
(76) Sun, Z.; Liu, R.; Su, T.; Huang, H.; Kawamoto, K.; Liang, R.; Liu, B.; Zhong, M.; Alexander-Katz, A.; Ross, C. A.; Johnson, J. A. Emergence of Layered Nanoscale Mesh Networks through Intrinsic Molecular Confinement Self-Assembly. *Nat. Nanotechnol.* **2023**, *18*, 273−280.
(77) Bonneau, C.; O'Keeffe, M. High-Symmetry Embeddings of Interpenetrating Periodic Nets. Essential Rings and Patterns of Catenation. *Acta Crystallogr. A Found. Adv.* **2015**, *71*, 82−91.
(78) Fredrickson, G. H. Desperately Seeking Soft Structures. *Proc. Natl. Acad. Sci. U.S.A.* **2023**, *120*, e2318123120.
(79) Dong, Q.; Gong, X.; Yuan, K.; Jiang, Y.; Zhang, L.; Li, W. Inverse Design of Complex Block Copolymers for Exotic Self-Assembled Structures Based on Bayesian Optimization. *ACS Macro Lett.* **2023**, *12*, 401−407.

https://doi.org/10.1021/acsmacrolett.4c00661
ACS Macro Lett. 2024, 13, 1612−1619